Advanced Composite Materials
Publication details, including instructions for authors and subscription information:
http://www.tandfonline.com/loi/tacm20

Effect of Reinforced Fiber Length on the Damping Performance of Thermoplastic Composites

C. Subramanian [a], Sunil Balwant Deshpande [b] & S. Senthilvelan [c]

[a] Department of Mechanical Engineering, Indian Institute of Technology Guwahati, Guwahati 781039, Assam, India

[b] Department of Mechanical Engineering, Indian Institute of Technology Guwahati, Guwahati 781039, Assam, India

[c] Department of Mechanical Engineering, Indian Institute of Technology Guwahati, Guwahati 781039, Assam, India;, Email: ssvelan@iitg.ernet.in

Version of record first published: 02 Apr 2012.

To cite this article: C. Subramanian, Sunil Balwant Deshpande & S. Senthilvelan (2011): Effect of Reinforced Fiber Length on the Damping Performance of Thermoplastic Composites, Advanced Composite Materials, 20:4, 319-335

To link to this article: http://dx.doi.org/10.1163/092430410X550872

///VSP///
Advanced Composite Materials 20 (2011) 319–335
ADVANCED COMPOSITE MATERIALS
brill.nl/acm

Effect of Reinforced Fiber Length on the Damping Performance of Thermoplastic Composites

C. Subramanian, Sunil Balwant Deshpande and S. Senthilvelan *
Department of Mechanical Engineering, Indian Institute of Technology Guwahati, Guwahati 781039, Assam, India

Received 24 June 2010; accepted 19 November 2010

Abstract
Discontinuous fiber reinforced thermoplastic materials are being used in many engineering applications. To widen their structural and antivibration application, there is a need to understand damping performance and its associated mechanisms. In this work, unreinforced, 20% short glass fiber reinforced and 20% long glass fiber reinforced polypropylene (PP) materials have been considered. Test materials were subjected to deformation to identify energy absorbing mechanisms and to quantify damping. Test specimens were also subjected to free and forced vibration to quantify structural damping characteristics, namely, damping factor and phase lag between excitation force and material response. Unreinforced material exhibited higher damping performance than reinforced composite material. Short fiber reinforced PP exhibited superior damping behavior than long fiber reinforced PP due to its high fiber end density and weak fiber matrix interface.

Keywords
Thermoplastic composite, damping, elastic hysteresis, phase lag, matrix interface

Notation

n	number of cycles
t	time lag in sec between exciting forcing and response
T	time period of one cycle
X_1	vibration amplitude of the first cycle
X_n	vibration amplitude after nth cycle
$\tan\delta$	loss factor
ω	forced exciting frequency

* To whom correspondence should be addressed. E-mail: ssvelan@iitg.ernet.in
Edited by the KSCM

 DOI:10.1163/092430410X550872

ω_n natural frequency

ξ damping factor

δ logarithmic decrement

ϕ phase lag

1. Introduction

In recent years, discontinuous fiber reinforced thermoplastic materials are finding many engineering applications due to their simple processing and superior mechanical properties. Fiber reinforcement in the polymeric material not only enhances strength and stiffness but also alters the damping characteristics of the composite. Enhanced stiffness along with good damping characteristics of discontinuous fiber reinforced thermoplastic materials are properties that suit many anti-vibration applications. Complete understanding of all the damping sources pertaining to the discontinuous fiber reinforced thermoplastic material would aid the design of these classes of materials suitable for the best utilization. Discontinuous fibers in the composite alter the damping characteristics owing to the presence of the fiber–matrix interfacial bond, voids and stress concentrations around fiber ends [1–3]. In a fiber reinforced composite, the characteristics of the fiber–matrix interface significantly alters the damping characteristics [2]. When a material is subjected to large amplitude of vibration/high stress levels, it exhibits non-linear visco plastic damping [3]. The damping characteristics of polymer composites are influenced by the effect of fiber volume fraction and fiber orientation. Adams and Maheri [4] proposed a model to understand the basic damping mechanisms of laminated composite plates, in which the damping capacity for various fiber orientations was computed theoretically and compared with experimental results. Test results revealed that damping capacity was maximum at an orientation of 45°. Crema *et al.* [5] evaluated the damping coefficient by exciting a cantilever test specimen made of short glass fiber reinforced thermoplastics with different fiber orientations: experimental results revealed that fibers orientated randomly possessed higher damping values than those of longitudinal and transverse orientations. Lee *et al.* [6] investigated the dynamic characteristics of carbon fiber reinforced polyether–ether–ketone through flexural and torsional vibration tests, in which the measured natural frequency and specific damping capacity were compared with finite element analysis results. Valtorta *et al.* [7] presented a method for measuring damping in flexural vibration of polymeric and metallic fibers, in which the structural damping was determined from the measurement of phase difference between excitation and motion. Hadi and Ashton [8] investigated the influence of fiber orientation on the damping properties of glass fiber epoxy material using a flexural resonance method at various frequencies and reported the increase in loss factor with the decrease in fiber volume fraction; the maximum value of the loss factor was reported for an orientation of 45°. Saurez *et al.* [9] reported the influence of fiber length on the damping characteristics in discontinuous aramid and boron fiber reinforced epoxy laminates and visualized that composite with low fiber aspect ratios promoted good damping characteristics. Wray *et al.* [10] used decaying free transverse vibration to quantify logarithmic decrement of the injection molded short glass fiber reinforced polypropylene and observed the reduction in logarithmic decrement with the increase in fiber volume fraction; in addition, with respect to fiber orientation, the logarithmic decrement was found to be high at 45°. Vaidya *et al.* [11] measured damping factor for compression molded discontinuous long fiber polypropylene in longitudinal and transverse direction and observed the change in damping factor to be negligible. Gupta *et al.* [12] investigated the various energy absorbing mechanisms of short glass fiber reinforced polypropylene from tensile test: plastic deformation of the matrix, debonding, and fiber pull-out. Kultural and Eryurek [13] evaluated fatigue performance of polypropylene with different percentages of calcium carbonate and confirmed that the filler content not only influences the fatigue performance but also the damping performance. Gassan and Bledzki [14] investigated jute fiber reinforced polypropylene and reported the influence of fiber matrix adhesion on dynamic modulus and specific damping capacity.

Many research works have been carried out to understand the influence of reinforced fibers on the damping behavior of thermoset and thermoplastic laminate materials [3–8] but few works [9–13] have been attempted to understand the damping mechanism of discontinuous fiber reinforced thermoplastic materials. Though sufficient work has been carried out to understand the influence of reinforced fibers on structural and damping behavior of polymer composites, the influence of reinforced fiber length towards damping performance of the thermoplastic composites were not investigated in the past. Hence, in this work, the damping mechanism with respect to the reinforced fiber length in the discontinuous fiber reinforced polymeric materials was identified and various parameters, namely, hysteresis area, logarithmic decrement, phase lag and damping factor were evaluated and utilized.

2. Test Materials

To understand the damping behavior of discontinuous thermoplastic composites, unreinforced polypropylene (UFPP), 20% long glass fiber reinforced polypropylene (LFPP) and 20% short glass fiber reinforced polypropylene (SFPP) procured from Saint Gobain have been considered. The base resin PP of LFPP and SFPP materials all have same molecular weight. According to the material supplier's data, silane type coupling agent has been used for the manufacturing of SFPP and LFPP pellets. Since both the investigated materials used the same type and amount of coupling agent, material behavior discussions were limited only to the fiber length. Test materials were injection molded into rectangular specimens of size ($120 \times 12 \times 3$ mm^3) and tensile test specimens pertaining to ASTM D 638 standard. Molding conditions are given in Table 1. Injection molded test specimens were burnt in muffle furnace at 600°C and the extracted fibers were observed under optical microscope to con-

Table 1.
Injection molding parameters for test specimens

Material	Zone-1 (°C)	Zone-2 (°C)	Zone-3 (°C)	Screw diameter (mm)	Injection speed (mm/s)	Injection pressure (bar)	Mold temperature (°C)
Unreinforced polypropylene	190	180	175	35	80	100	30
20% short glass fiber reinforced polypropylene	220	205	200	35	75	100	30
20% long glass fiber reinforced polypropylene	240	235	235	35	65	110	30

firm the final fiber length in the molded specimens (Fig. 1). Length of the extracted fibers is measured using a Zeiss microscope (KS 300) with an image analysis system. Figure 2 shows the histogram of measured fiber length distribution. Weight average fiber length of the chosen SFPP and LFPP are 0.440 and 1.251 mm, respectively.

3. Hysteresis Damping

In general, viscous component of the matrix material significantly contributes to the hysteresis energy dissipation, which is identified as the major damping source of a thermoplastic material. To quantify damping due to the viscous component, load is applied on the molded tensile test specimens up to 500 N and released back to zero at the rate of 7.5 N/s using a servo-hydraulic machine (Instron 8801). Mantena *et al.* [15] used a similar method to obtain the hysteresis loop and evaluate the damping performance for pultruded beams. Figure 3 shows the hysteresis area which is formed by the load–deflection curve during loading and unloading and quantifies the dissipated energy within the material per unit cycle. The hysteresis areas of UFPP, SFPP and LFPP are found to be 110.85, 30.48 and 25.57 Nmm, respectively. The area formed by this loop indicates the hysteresis damping of the chosen test materials, which is partly stored in the microstructure (crazes, shear bands, voids and micro cracks) and partly dissipated as heat. Unreinforced polypropylene (PP) exhibited a higher area than that of reinforced PP. Among reinforcement material, SFPP exhibited a higher hysteresis area than LFPP due to the presence of more fiber ends/fiber matrix interface area. For the fixed volume fraction of reinforcement, due to the higher fiber ends and fiber matrix interface area (Fig. 4), short fiber reinforced material exhibited superior damping characteristics than that of long fiber reinforced material.

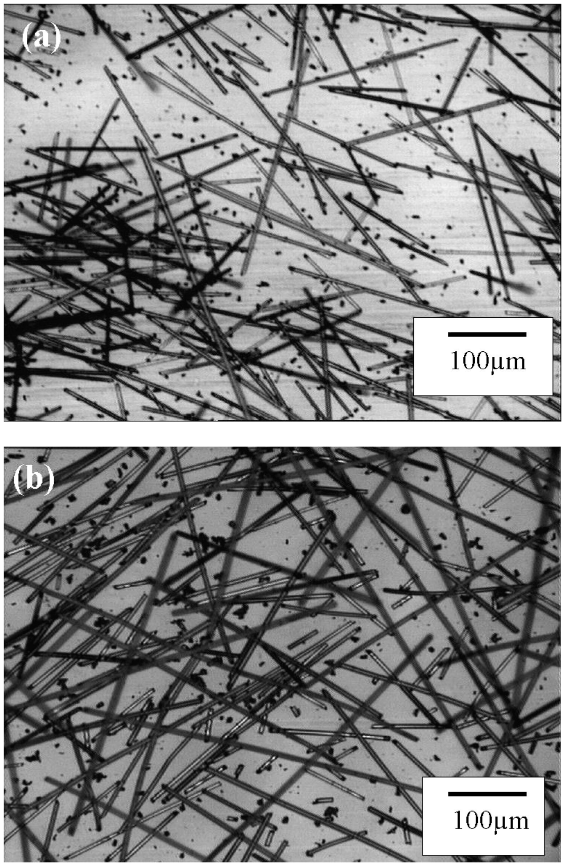

Figure 1. Separated fibers from test specimens (a) short fiber reinforced polypropylene and (b) long fiber reinforced polypropylene.

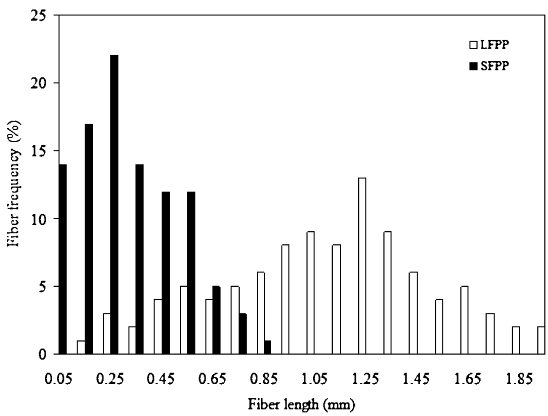

Figure 2. Fiber length distribution of long and short fiber reinforced polypropylene.

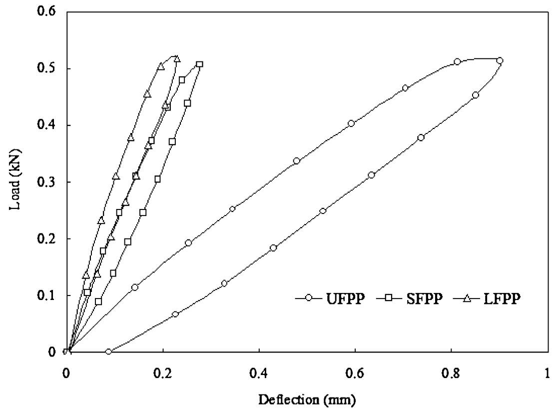

Figure 3. Hysteresis loop of unreinforced and reinforced polypropylene during constant load test.

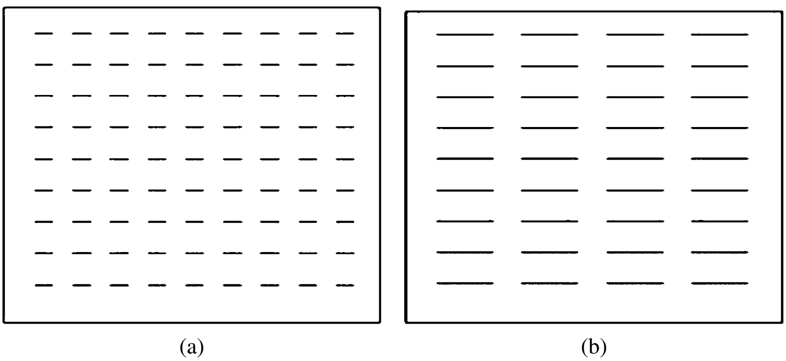

Figure 4. Schematic of fibers in a matrix for the same volume fraction (a) short fiber reinforced polymer and (b) long fiber reinforced polymer.

4. Damping due to Fiber–Matrix Interface

In the composite, the interface between reinforced fiber and the supporting matrix is identified as one of the most significant sources of damping. In general, the ideal interface plays the role of transferring the entire load and does not therefore contribute to the damping characteristics [2]. To quantify damping due to fiber–matrix interface, tensile tests were carried out on chosen materials and fractured surfaces have been investigated to understand the fiber–matrix interface. All the tests were performed under atmospheric conditions (23°C and 50% humidity). The gauge length of the test material was 50 mm and the crosshead was moved up with the speed of 1 mm/min. Figure 5 shows the stress–strain curve of the test materials. Addition of reinforcement increases material modulus and strength. SFPP exhibited more fiber pull out failures, whereas LFPP shows very less/no fiber pull out (Figs 6 and 7). Thus increase in fiber length of LFPP material accounts for more surface area of the fiber and provides good interfacial bonding strength with the matrix and thus fiber pullout is avoided and matrix deformation was visualized. In the interfacial

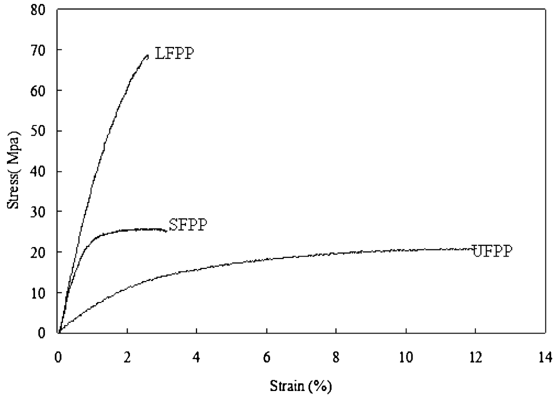

Figure 5. Stress–strain curve of unreinforced and reinforced polypropylene.

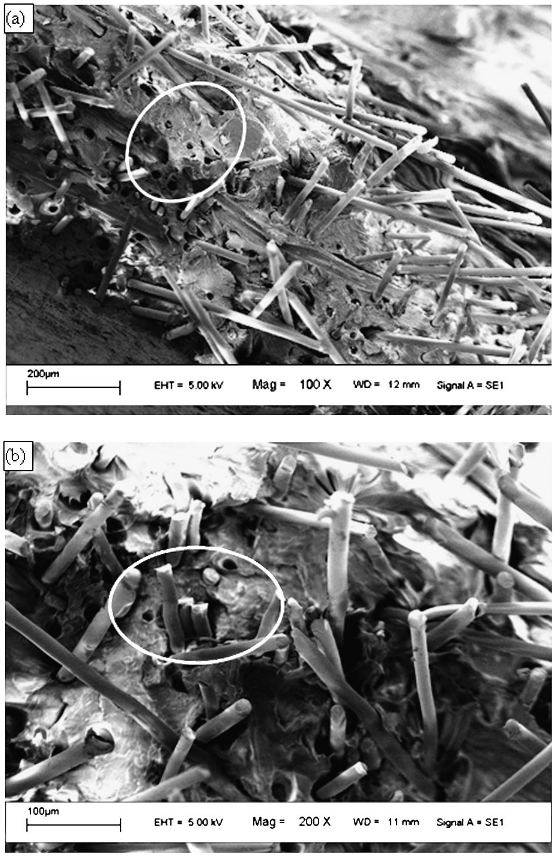

Figure 6. (a) and (b) Fractured surface of short fiber reinforced polypropylene test specimen showing more fiber pullout failure.

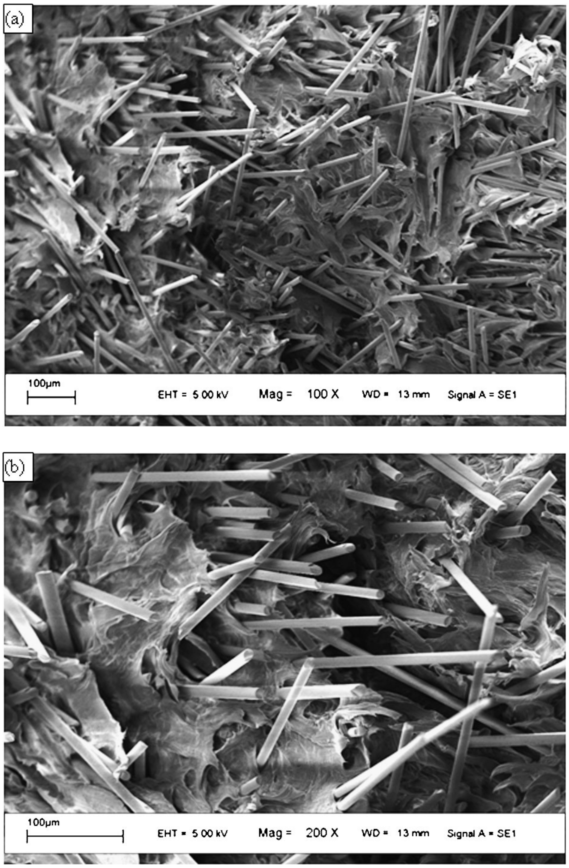

Figure 7. (a) and (b) Fractured surface of long fiber reinforced polypropylene test specimen showing no fiber pullout failure.

bonding of fiber and matrix, the region near the fiber end is the weakest region and hence more energy is absorbed in this region, which contributes to increase the damping. SFPP materials exhibited more fiber ends than that of LFPP for the same volume fraction of the reinforcement (Fig. 4). Because there were more fiber ends, damping due to the fiber–matrix interface was higher in the SFPP than that of LFPP. The higher strength and modulus of LFPP also confirms that there were fewer fiber pullouts and less fiber–matrix debonding. Gassan and Bledzki [14] reported that composite having good fiber–matrix adhesion exhibited less specific damping capacity than composite with poor fiber–matrix adhesion.

5. Damping under Free Vibration

Energy dissipation through plastic and elastic deformation is neglected when the test specimens are subjected to free vibration. A schematic arrangement for the free transverse vibration testing of the test specimen is shown in Fig. 8. The specimen

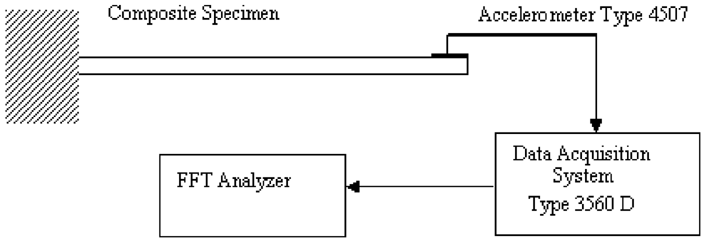

Figure 8. Schematic arrangement of experimental setup for free vibration condition.

(120 × 12 × 3 mm) is clamped at one end, and an accelerometer (Bruel and Kjaer, Type 4507) is fixed at the end of the cantilever beam. The initial specimen displacement is caused with an impact hammer. Free end displacement of the specimen is measured and recorded with an accelerometer and finally fed in to the data acquisition system. Many works have been reported in the past using similar methodology for the evaluation of damping factor [7–11]. The procedure is repeated for all the three test materials. From the time domain data, the decay rate of free oscillation is measured by the logarithmic decrement (δ):

$$\delta = \frac{1}{n-1} \ln\left(\frac{X_1}{X_n}\right), \tag{1}$$

where n is the number of cycles, vibration amplitude of the first cycle is X_1 and vibration amplitude after the nth cycle is X_n. The damping factor (ξ) is calculated from the logarithmic decrement (δ) using the equation:

$$\delta = \frac{2\pi\xi}{\sqrt{1-\xi^2}}. \tag{2}$$

This procedure does not involve any complex signal processing technique, as the amplitude ratio can be obtained directly from the time domain data. Transient time decay curves are shown in Fig. 9. The logarithmic decrement values of LFPP, SFPP and UFPP are 0.2255, 0.3645 and 0.4154, respectively, and the corresponding damping factors pertaining to LFPP, SFPP and UFPP materials are found to be 0.0359, 0.0579 and 0.0659, respectively. Wray *et al.* [10] reported the reduction of logarithmic decrement and damping factor with the increase in fiber volume fraction. The presence of more fiber ends contributes to improve damping in SFPP as discussed in the previous section. Damping performance of the chosen test materials also exhibited similar trend as indicted by the hysteresis area.

6. Damping under Forced Vibration

Energy dissipation through plastic deformation is neglected when the test specimens are subjected to forced vibration. Schematic and experimental arrangements for the forced transverse vibrations of the composite specimen are shown in Fig. 10(a) and 10(b), respectively. The test specimen is clamped at one end and

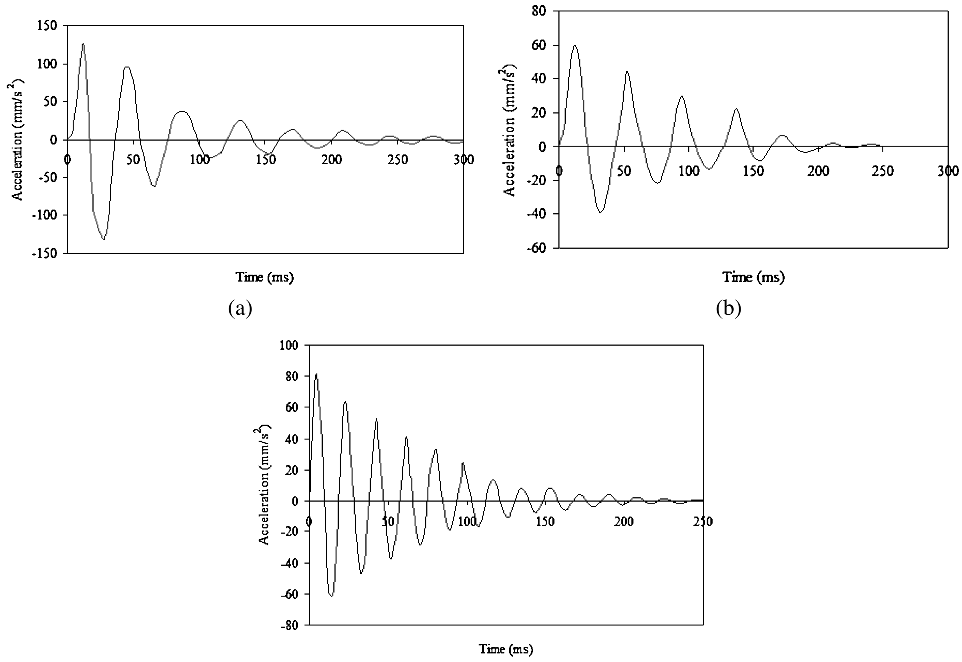

Figure 9. Decay curve of (a) unreinforced material, (b) short fiber reinforced material and (c) long fiber reinforced material.

the force transducer (Bruel and Kjaer, 8230-001) is fixed above the exciter and connected at the other end. An accelerometer is fixed at free end and the signals from the accelerometer and force transducer are measured and stored with respect to time. The exciter (Bruel and Kjaer, 4824) is vibrated at a sinusoidal exciting frequency of 20 Hz. The schematic of exciting force and its response is shown in Fig. 11 and the phase lag is calculated using following relation:

$$\phi = \frac{t}{T} \times 360^\circ, \tag{3}$$

where T is the time period of one cycle and t is time lag in seconds between exciting forcing and response. Three trials were conducted for all the materials**.** Phase lag is the time by which the response lags behind the exciting force and it is a measure of the damping. Valtorta *et al.* [7] have also determined structural damping of fibers by measuring the phase difference between excitation and motion. For a material, phase lag is directly proportional to the damping [16, 17], i.e., higher phase lag angle indicates higher material damping. Damping factor from forced vibration is calculated using the following relation [18]:

$$\tan\phi = \frac{2\xi(\omega/\omega_\mathrm{n})}{1-(\omega/\omega_\mathrm{n})^2}, \tag{4}$$

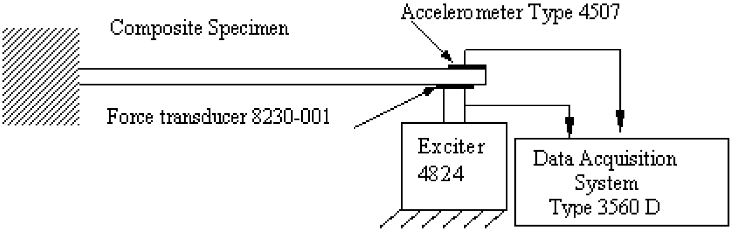

(a)

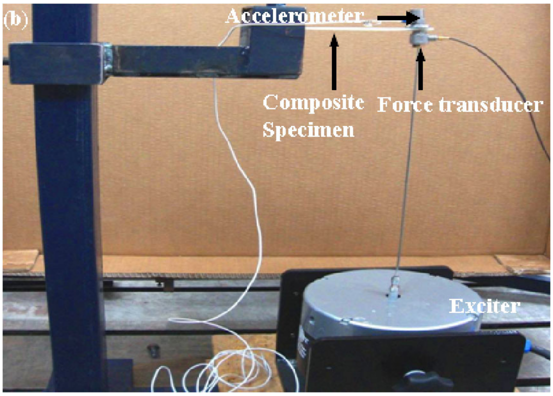

Figure 10. (a) Schematic diagram of experimental setup for forced vibration condition. (b) Photograph of experimental setup for forced vibration condition. This figure is published in color in the online version.

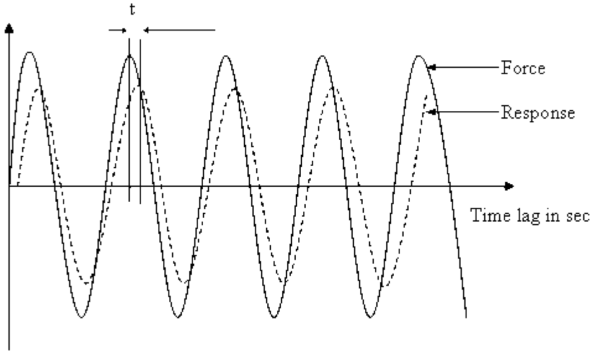

Figure 11. Schematic of excitation force and its response.

where ϕ is the phase lag angle, ω is the forced exciting frequency (20 Hz) and ω_n is the natural frequency. The natural frequency for UFPP, SFPP and LFPP obtained for the specimen from the Fast Fourier Transform (FFT) analyzer during the free vibration are shown in Fig. 12(a)–(c). The phase lag obtained from the forced vibration experiment for the all the considered test specimens is shown in Fig. 13(a)–(c). Figure 14 shows the mean phase lag of all the considered test specimens. The deviations of the determined mean phase lag are found to be well within 3%. Phase lag

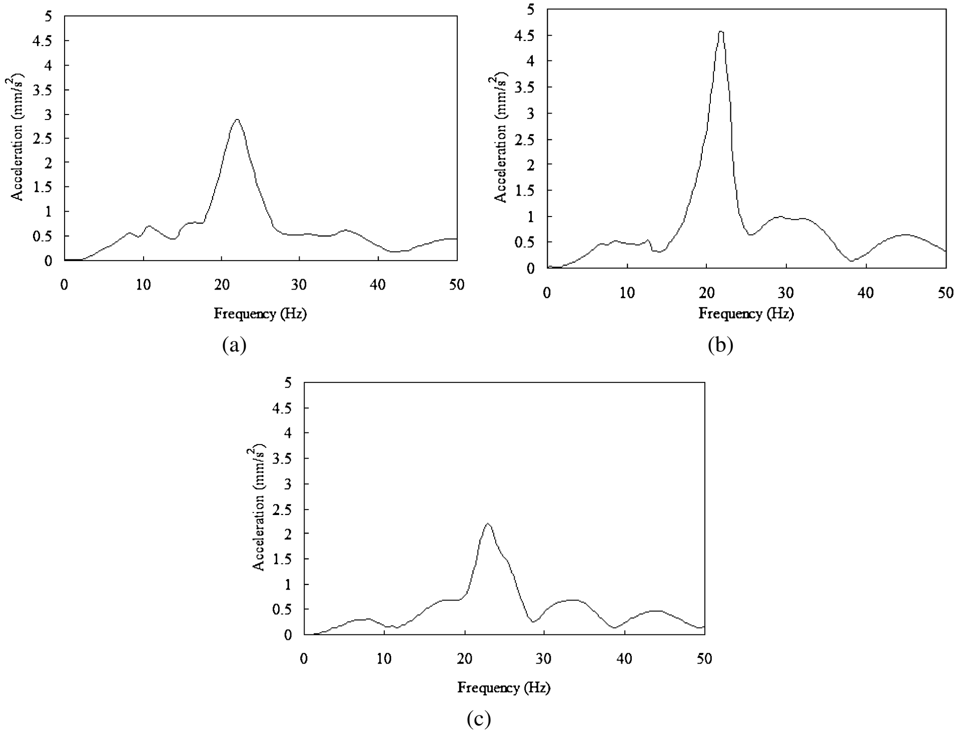

Figure 12. Vibration signal from FFT analyzer for specimen showing the natural frequency for (a) unreinforced PP, (b) short fiber reinforced PP and (c) long fiber reinforced PP.

of unreinforced, short fiber reinforced and long fiber reinforced PP materials are 31.56°, 28.46° and 27.69°, respectively. Addition of reinforced fibers to the base polypropylene significantly limits the material elastic deformation and decreases the phase lag between the exciting force and the corresponding material response. Among reinforced material, SFPP showed increased phase lag compared to that of LFPP due to the presence of more fiber matrix interface, which ultimately delayed initiation of the response. The calculated damping factors obtained from the forced vibration test for LFPP, SFPP and UFPP are 0.0393, 0.0517 and 0.0644, respectively. Since the test specimen geometry and air damping conditions are similar in both free and forced vibration technique, the obtained damping factors are almost the same. The damping factor and phase lag obtained from forced vibration tests exhibited similar trend to that of the hysteresis area and the logarithmic decrement obtained through free vibration tests.

7. Damping under Dynamic Mechanical Analysis

In the structural applications, materials are often being subjected to dynamic loads under various temperatures; hence, exploration of damping performance under forced vibration at various temperatures helps to design these materials suitably.

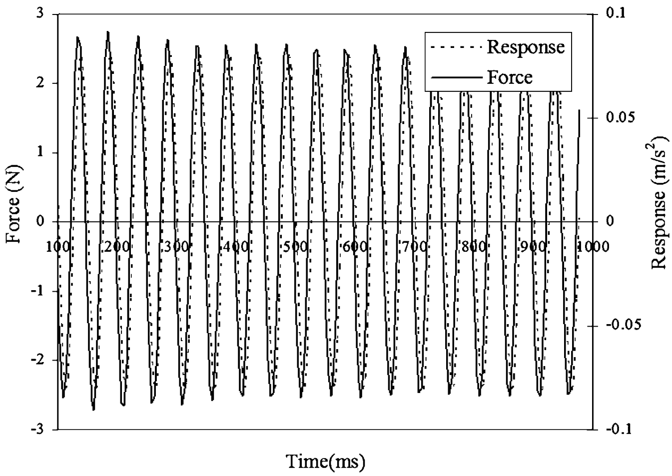

(a)

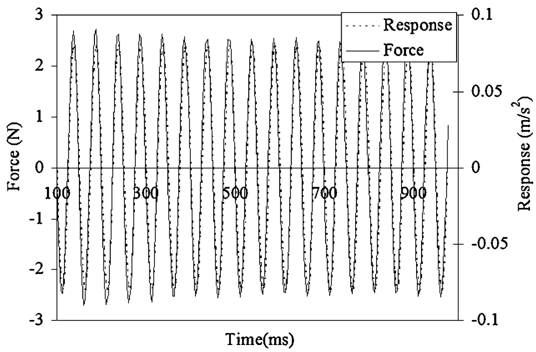

(b)

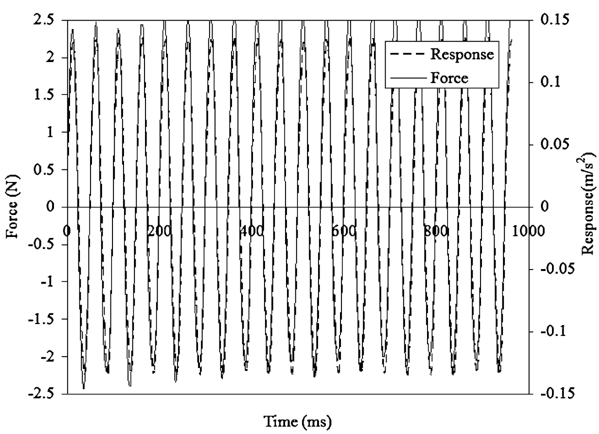

(c)

Figure 13. Phase lag plot between excited force and its response for (a) unreinforced material, (b) short fiber reinforced material and (c) long fiber reinforced material.

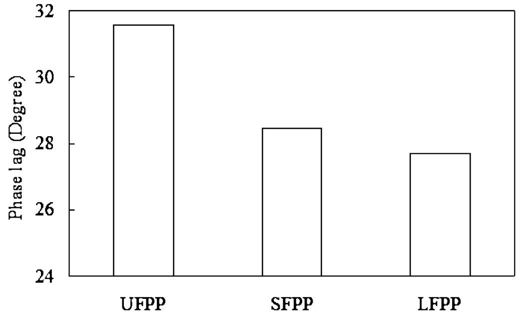

Figure 14. Phase lag between excited force and its response of the test specimens.

So the chosen test materials have been subjected to dynamic mechanical analysis. Dynamic mechanical analysis (DMA) is carried out on the injection molded test specimens pertaining to ASTM D6382 standard using Perkin-Elmer, DMA/7E. Test specimens were subjected to bending in a cantilever mode with a span length of 70 mm. An oscillatory force of 3 N is applied over a temperature range of 32–92°C. The scan was performed at a frequency of 0.1 Hz. Figure 15(a)–(b) shows the variation of storage modulus and loss modulus of test materials as a function of temperature, tested at 1 Hz frequency. It is very evident that the increase in the fiber length of reinforcement improves the material stiffness at dynamic condition. The storage modulus and loss modulus of LFPP material is found to be high compared to that of UFPP and SFPP materials. Since the mean fiber length of LFPP (1.251 mm) is larger than that of SFPP (0.4403 mm), the molecular mobility of LFPP polymer matrix is restricted which results in superior modulus. Loss factor ($\tan\delta$) is obtained by considering the ratio between loss modulus and storage modulus. The loss factors of the chosen materials, LFPP, SFPP and UFPP at room temperature are found to be 0.062, 0.068 and 0.087, respectively (Fig. 15(c)). The damping factor is calculated using the relation [19]:

$$\xi = \frac{\tan\delta}{2}. \tag{5}$$

The computed damping factors of LFPP, SFPP and UFPP at room temperature are 0.031, 0.034 and 0.0435, respectively (Fig. 15(c)). However, the damping factors obtained from the free vibration test for the LFPP, SFPP and UFPP are 0.0359, 0.0579 and 0.0659, respectively. This variation is due to the change in specimen geometry and condition of air damping [17]. It is to be noted that the specimen size used for DMA ($70 \times 13 \times 3$ mm^3) was smaller than specimen size used in the free vibration test ($120 \times 12 \times 3$ mm^3). Due to this, the clamping area is also altered; in addition, the free vibration was carried out in open condition (wherein air damping was present) whereas DMA involved a closed chamber for evaluating the loss factor. The damping factor dropped with the increase in fiber length. The restriction of polymer molecules due to the presence of high modulus fibers has caused the reduction in damping factor in polypropylene composites [20]. Rezaei *et al.* [21] also

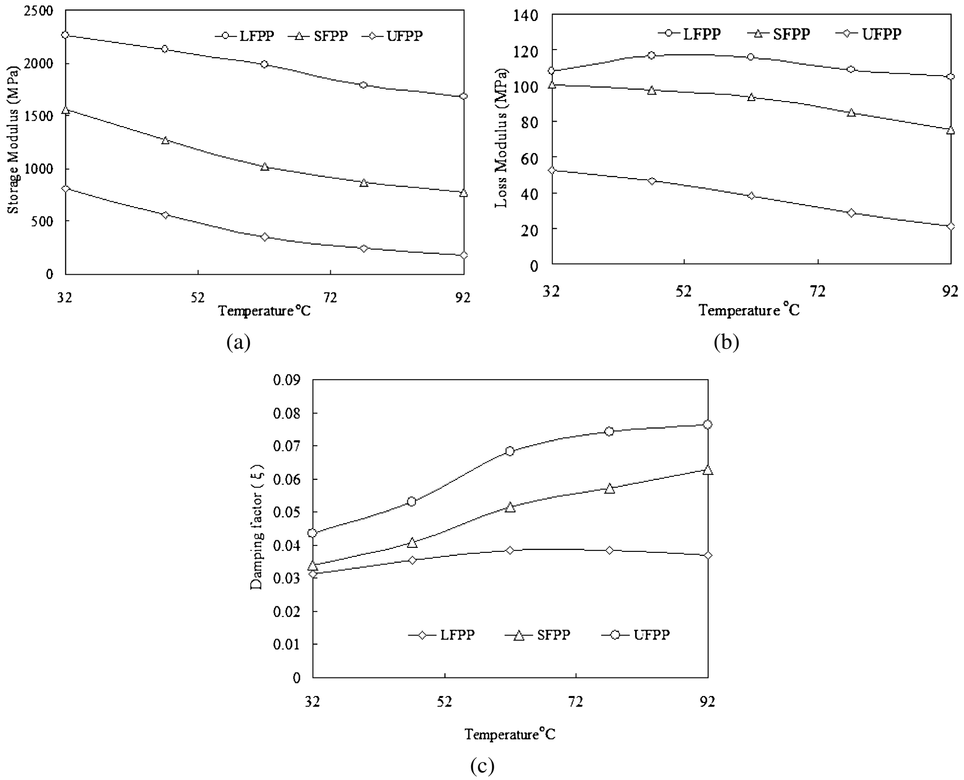

Figure 15. Dynamic mechanical analysis of polypropylene composites showing (a) storage modulus with respect to temperature, (b) loss modulus with respect to temperature and (c) damping factor with respect to temperature.

observed loss factor reduction in carbon fiber reinforced polypropylene composites with the increase in fiber length. The damping factor of all the chosen test materials increases with the increase in temperature, this behavior is due to the matrix softening which resulted in molecular mobility increase at elevated temperature. When the test material temperature increases, the free volume, i.e., space for the internal movement of the molecule increases, which results in drop of storage modulus and loss modulus and hence increase in damping factor is observed. The increase in damping factor with increase in temperature is less for LFPP due to the reinforcing efficiency of longer glass fiber polypropylene composites in retaining the modulus at higher temperatures. Thomason and Groenewoud [22] also observed similar performance for glass fiber polypropylene composites at higher temperatures.

8. Conclusions

The damping performance of UFPP, SFPP and LFPP has been evaluated through different techniques, namely, material deformation (elastic and plastic), free vibration, forced vibration and dynamic mechanical analysis. In spite of a similar damping performance trend (UFPP > SFPP > LFPP) exhibited by the test materials, the respective damping parameters (hysteresis area, logarithmic decrement, phase lag and damping factor) imply different damping mechanisms in the discontinuous fiber reinforced thermoplastic materials.

Different sources of energy dissipation in discontinuous fiber reinforced composites have been correlated with respect to the reinforced fiber length and the following major conclusions have been drawn:

1. When test materials are being subjected to elastic as well as plastic deformation, the fiber–matrix interface is identified as a major source of material damping. Unreinforced material exhibited higher hysteretic area than reinforced material. Among reinforced material, SFPP exhibited higher energy dissipation than that of LFPP due to the presence of more fiber ends and fiber–matrix interfaces.

2. When test materials are being subjected to free vibration, logarithmic decrement and damping factor were found to decrease with the increase in fiber length. When the test materials are being subjected to forced vibration, damping to plastic deformation is neglected. SFPP exhibited higher phase lag between the excited force and its response than that of LFPP material.

References

1. D. J. Nelson and J. W. Hancock, Interfacial slip and damping in fiber-reinforced composites, *J. Mater. Sci.* **13**, 2429–2440 (1978).
2. R. Chandra, S. P. Singh and K. Gupta, Damping studies in fiber-reinforced composites — a review, *Compos. Struct.* **46**, 41–51 (1999).
3. J. M. Kenny and M. Marchetti, Elasto-plastic behavior of thermoplastic composite laminates under cyclic loading, *Compos. Struct.* **32**, 375–382 (1995).
4. R. D. Adams and M. R. Maheri, Damping in advanced polymer–matrix composites, *J. Alloy Compounds* **355**, 126–130 (2003).
5. L. B. Crema, A. Castellani and A. Serra, Experimental tests for damping measurement on several short glass fiber composites, *J. Compos. Mater.* **23**, 978–987 (1989).
6. I. Lee, B. N. Kim and K. N. Koo, Dynamic characteristics of thermoplastic composite laminates, *Composites* **25**, 281–286 (1994).
7. D. Valtorta, J. Lefevre and E. Mazza, A new method for measuring damping in flexural vibration of thin fibers, *Exper. Mech.* **45**, 433–439 (2005).
8. A. S. Hadi and J. N. Ashton, Measurement and theoretical modeling of the damping properties of a unidirectional glass/epoxy composite, *Compos. Struct.* **34**, 381–385 (1996).
9. S. A. Saurez, R. F. Gibson, C. T. Sun and S. K. Chaturvedi, The influence of fiber length and fiber orientation on damping and stiffness of polymer composite materials, *Exper. Mech.* **26**, 175–184 (1986).
10. S. Wray, J. N. Ashton and H. El-Sobky, An investigation of the influence of anisotropy and frequency on damping in short glass fiber reinforced polypropylene, *Compos. Struct.* **15**, 43–60 (1990).
11. U. K. Vaidya, A. Goel and K. Chawla. Fatigue and vibration response of long fiber reinforced thermoplastics, in: *Automotive Composites Conference and Exhibition, SPE*, USA, pp. 1–6 (2009).

12. V. B. Gupta, R. K. Mittal and G. Malti, Energy absorbing mechanisms in short glass fiber reinforced polypropylene, *Compos. Sci. Technol.* **37**, 353–368 (1990).
13. S. E. Kultural and I. B. Eryurek, Fatigue behavior of calcium carbonate filled polypropylene under high frequency loading, *Mater. Des.* **28**, 816–823 (2007).
14. J. Gassan and A. K. Bledzki, Possibilities to improve the properties of natural fiber reinforced plastics by fiber modification — jute polypropylene composites, *Appl. Compos. Mater.* **7**, 373–385 (2000).
15. P. R. Mantena, J. G. Vaughan, R. P. Donti and M. V. Kowsika, Influence of process variables on the dynamic characteristics of pultruded graphite–epoxy composites, in: *Proc. Vibro-Acoustic Characterization of Materials and Structures*, ASME, California, USA, pp. 147–154 (1992).
16. J. Aberg and B. Widell, Uniaxial material damping measurements using a fiber optic lattice: a discussion of its performance envelope, *Exper. Mech.* **44**, 33–36 (2004).
17. K. P. Menard, *Dynamic Mechanical Analysis: A Practical Introduction*. CRC Press, Florida, USA (1999).
18. G. Genta, *Vibration of Structures and Machines*. Springer Verlag, New York, USA (1999).
19. L. D. Landro, and W. Lorenzi, Mechanical properties and dynamic mechanical analysis of thermoplastic–natural fiber/glass reinforced composites, *Macromol. Symp.* **286**, 145–155 (2009).
20. B. Harris, O. Braddel, D. Almond, C. Lefebure and J. Verbic, Study of carbon fiber surface treatment by dynamic mechanical analysis, *J. Mater. Sci.* **28**, 3353–3366 (1993).
21. F. Rezaei, R. Yunus and N. A. Ibrahim, Effect of fiber length on thermo mechanical properties of short carbon fiber reinforced polypropylene composites, *Mater. Des.* **30**, 260–263 (2009).
22. J. L. Thomason, and W. M. Groenewoud, The influence of fibre length and concentration on the properties of glass fibre reinforced polypropylene: 2. Thermal properties, *Composites Part A* **27**, 555–565 (1996).